Updating land use and land cover classes of Blue Nile basin using landsat-8 images

Updating land use and land cover classes of Blue Nile basin using landsat-8 images

A S Shobary[1], A Elsharkawy[1], H E M El-Hanafy[1] and O M Moussa[1]

[1]Department of Civil Engineering, Military Technical College, Cairo, Egypt.

E-mail: a.s.shobary@mtc.edu.eg

Abstract. Land Use and Land Cover are considered as a main input layer for the estimation of surface runoff along with the soil maps, rainfall data, DEM. The main purpose of this research paper is to update the Land Cover and Land Use of the Blue Nile basin that can be used for further processing to estimate the surface runoff of the Blue Nile basin. Recent satellite images of Landsat 8, dated May and June, 2020, were used with less than 10% clouds covering the full scene of the study area. Six land cover classes were targeted namely; water, urban, barren land, forest, grass and agricultural crops. Supervised (maximum likelihood) classification method was used and accuracy assessment with the help of google earth as ground truth was performed. With the aid of 30-m DEM, the Blue Nile basin was divided into fourteen sub-watersheds. Classification scheme was applied to each of the fourteen sub-watersheds and the classification results were introduced as a percentage of the total area of each sub-watershed. Moreover, confusion matrices were formed for the sub-watersheds.

1. Introduction

Image classification is the method used to generate thematic maps from imagery. For example, the themes may vary from layers like surface water, soil and vegetation in the general characterization of a rural region, to specific sorts of vegetation, soil and pureness or depth of water for a more comprehensive description.

The process of possession descriptive labels, which classes various surface materials and conditions, is the prospective and final result. The data have been probably translated into a form that has information meaning by virtue of the labelling process [1].

Land Use and Land Cover are considered as a main input layer for the estimation of surface runoff along with the soil maps, rainfall data, DEM. The main purpose of this research paper is to introduce a recent update to the Land Cover and Land Use of the Blue Nile basin that can be used for further processing to estimate the surface runoff of the Blue Nile basin.

Abbay basin, area of study, is located in northwest of Ethiopia. Its average annual runoff was estimated about 54.8 BCM [2]. Lake Tana is considered the main head of Abbay basin. With the help of 30-m resolution DEM, Geographic Information System(GIS) was used to delineate Abbay basin and divide it into fourteen sub watersheds.

Landsat-8 images were used in this study as they are freely available. They were downloaded from Earth Explorer Web browser and georeferenced to the Universal Transverse Mercator map projection (World Geodetic System, WGS 84 datum, UTM Zone 37 N). These images were captured in the dry season with less than 10% cloud cover.

Most classes of land cover, identified by remote sensing, are organized by classification scheme [3]. In this study, six land cover classes were targeted and plotted in the scheme as water, urban, barren land, forest, grass and agriculture crops.

Supervised (maximum likelihood) classification was used to make the required thematic map. Training samples were drawn on the images and ground truth were featured with the help of google earth. This operation was repeated for the whole thirteen sub watersheds.

In this study, Environment for Visualizing Images (ENVI) was used to create confusion matrices for the whole sub watersheds and estimate measures of classification accuracy: user's accuracy, producer's accuracy and overall accuracy.

Objective of this study is to produce updated thematic maps of land use and land cover of the Blue Nile Basin that can be recently used for estimating surface runoff.

2. Area of Study

The Nile River is considered the longest one in the world with total length of 6670 km. The river drains a catchment with area of 3.4 million km2. There are two main tributaries feeding The Nile, the White Nile and Blue Nile. The White Nile originates from The Equatorial Lakes plateau in Uganda and meets the Blue Nile, which rises from the Ethiopian Highlands, at Khartoum. The Nile River has another main tributary, Atbara River, originating from the Ethiopian Plateau to the north of Khartoum where it joins the main Nile [4].

The Blue Nile Basin and its main tributaries drain an estimated area of 324,000 km^2, about 250,000 km^2 in the Ethiopian Plateau. The Blue Nile Basin is divided into two parts; the part in Ethiopia called Abbay Basin or Ethiopia-Blue Nile, situated in the northwestern district of Ethiopia. The Blue Nile Basin exists between 34^0 $0^{'}$ $25^{"}$ E and 39^0 $0^{'}$ $49^{"}$ E longitude, and 7^0 $0^{'}$ $40^{"}$ N and 12^0 $0^{'}$ $51^{"}$ N latitude. There are other four basins have common boundaries with Blue Nile Basin: Tekeze basin in the north, the Awash basin in the east and south east, the Omo-Gibe basin in the south, and the Baro-Akobo basin in the south west. The main head of the Blue Nile (Abbay) river, Lake Tana, the greatest freshwater lake in the country is situated in the north part of the basin[5].

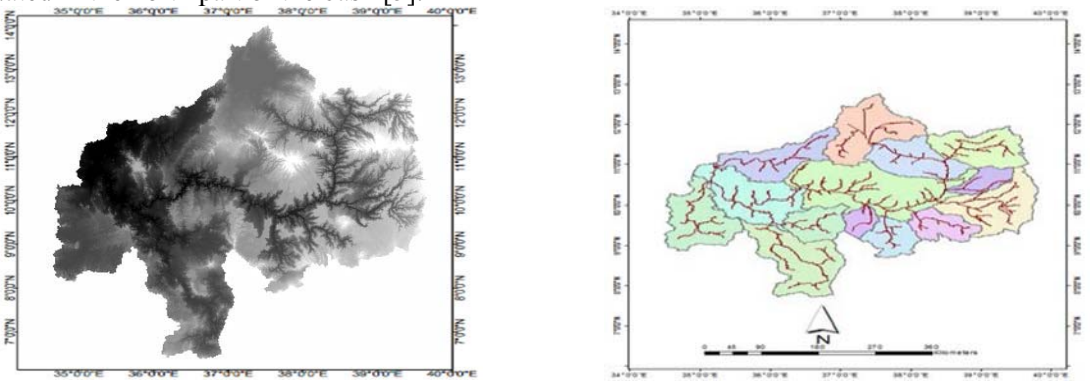

a) Mosaicked DEM of Blue Nile basin b) Watersheds forming the Blue Nile basin

Figure 1 Location of study area

Figure 1 shows transformation of DEM of study area (remote sensing data) into 14 sub watersheds by Arcgis. Area of sub watersheds, forming the study area, is illustrated in the following table.

Table 1. Area of sub watersheds.

Watershed	Beshelo	Tana	Jemma	Weleka	Mugger	Guder	South Gojam
Area (km^2)	12085	15935	15248	4448	6907	6594	27635
Watershed	Anger	Wenbera	Didessa	Dabus	Beles	Fincha	North Gojam
Area (km^2)	7475	16859	17855	13716	12327	3308	12045

South of lake Tana, a small spring which is considered the main source of the Blue Nile drains at height 2900 m and approximately 100 km length. The Abbay basin has a main portion in the irrigation and hydropower potential of Ethiopia with 815,581 ha and 78,820 GWH/yr respectively. Awlachew et.al estimated an average annual runoff of the basin about 54.8 BCM [2].

The Abbay Basin consist of 14 sub watersheds as shown previously in Figure 1. There are two unlike features form the topography of the Abbay basin; in the center and the eastern part, amorphous mountains areas form the highlands and the lowlands exist in the western part of the basin. The Ethiopian Plateau rises at elevations ranges from 1500 m up to 4000 m above mean sea level with average slope more than 25% in the eastern part, highlands, whereas the lowlands in the west prostrates 1000 m to 500 m above mean sea level with average slope less than 7%. Latitude, altitude, slope and exposure are factors that affect the climate of Abbay basin. The duration from June to September form the rainy season [6].

The large amount of rainfall is concentrated in the Ethiopian highlands ranging from 1500 to 2200 mm with peaks in August, on the other hand, the rainfall in the lowlands is less than 1500 mm. The climate of the basin differs from one region to another. The western part possesses the highest temperature with maximum and minimum range 280C-380C and 150C-200C respectively. In the eastern and central basin's part, lower temperature is monitored. The maximum temperature extents 120C – 200C whereas the minimum being -10C to 80C. There is an interconnection between temperature and potential evapotranspiration. In the lowlands, high temperature, high potential evapotranspiration ranging between 1800 mm and 2232 mm per year, lower potential evapotranspiration is observed between 1200 and 1800 mm per year in the eastern and southern parts. The highlands, lowest temperature, has the least potential evapotranspiration below 1200 mm per year [4].

Most of the study area is covered with volcanic materials, which are greatly common in the north central highlands in Ethiopia. Referring to uninterrupted events of storms through the rainy season, tough erosion is occurred, so the composition of these volcanic materials has a main significance for hydrologists and engineers. Huffnagle(1961) characterized two major types of siol: the black soils and the red to reddish browny clayey loams [7].

In depressions of the study area, the black soil exists. This type of soil is resulted from dolerites decay and is trended to fast crack and dry out. The red soil is greatly permeable. In the Blue Nile basin, there are various types of soil which differ from fine granular to medium or coarse. The fine granular has slow and moderate permeability but the medium and coarse has very slow one [8].

3. Methodology

3.1. Satellite image data sets

There are many factors for the choice of the most convenient satellite image data sources such as; images cost and availability of funding, available long time image series to analyze the change dynamics of the land cover and the area can be covered by suitable image data. According to the above criteria, Landsat 8 was found to be the most appropriate satellite to be used in this study. On February 11, 2013, Landsat 8 or Landsat Data Continuity mission, LDCM, was launched from Vandenberg Air Force Base, California, carried the Atlas-V vehicle. The Operational Land Imager, OLI, and the Thermal Infrared Sensor, TIRS, are the two sensors that installed on the satellite payload. OLI instrument develops pictures at nine wavelengths operating in the domain of 0.43-2.29 μm. Images that possessed from OLI instrument is at 15 m resolution so, they have a main role in studying many fields such: water quality control and cirrus clouds studying. TIRS acquires imagery at two infrared wavelengths with resolution of 100 m. The features of the image data are termed in Table 2.

Table 2. Landsat OLI and TIRS sensor system features [9].

sensor	Band number	Band name	Wavelength(μm)	Resolution
OLI	1	Coastal	0.43-0.45	30 m

OLI	2	Blue	0.45-.051	30 m
OLI	3	Green	0.53-0.59	30 m
OLI	4	Red	0.63-0.67	30 m
OLI	5	NIR	0.85-0.88	30 m
OLI	6	SWIR 1	1.57-1.65	30 m
OLI	7	SWIR 2	2.11-2.29	30 m
OLI	8	Pan	0.50-.68	15 m
OLI	9	Cirrus	1.36-1.38	30 m
TIRS	10	TIRS 1	10.60-11.19	100 m
TIRS	11	TIRS 2	11.50-12.51	100 m

All products of Satellite 8, including images used in this study, were corrected and georeferenced to the Universal Transverse Mercator map projection (World Geodetic System, WGS 84 datum, UTM Zone 37 N). These images are freely obtainable and can be downloaded from the United States Geological Survey, USGS, Earth Explorer web browser. To avoid cloud cover, these imags were acquired in the dry season. Less than 10% clouds cover the full scene of the study area as the images acquired in May and June,2020 (dry season).

3.2. Image pre-processing

Land sat images used in this study were of level 1 (on-demand imagery). A single multi-band image obtained by stacking the reflective bands with attached image file format (band 2, 3, 4, 5). After stacking layers of images, it was essential to mosaic these images to form the full scene of the study area as show in **Figure 2**. To simplify land cover analysis processing, the study area (Abbay basin) was divided into 14 sub-basins by importing shape file (vector) from **ArcGIS10.3**. Land cover classification was applied to each sub-basin separately.

Figure 2 Land sat images of Blue Nile basin

3.3. Classification scheme

Adequate attention must be paid to classification scheme used in such planning project that includes remotely sensed data. It is important for such classification scheme to be exclusive and in detailed [10].USGS, European Coordination of Information on the Environment (CORINE), and Africover used remote sensing data for developing classification systems. However, land use and land cover have no typical classification [11]. USGS Level I classification scheme is the basic and fundamental for organizing most types of land cover which had been identified by remote sensing [3]. For classification, in this study, six land cover classes were plotted in the scheme as water, urban, barren land, forest, grass and agricultural crops. Table 3 describes in detail the land cover classes.

Table 3. Land cover classes established and their description after [9].

Land cover class	description

Water	Including lakes, ponds, rivers and other open water areas.
Urban	Residential, commercial and industrial buildings are components of urban category.
Barren land	Sand, rocks and any land surface free of vegetation.
Forest	Trees, bushes, shrubs and any woody vegetation.
Grass	Areas covered by herbaceous vegetation.
Agricultural crops	Farms and bare crop fields.

3.4. Image classification

Land cover maps are produced from combination of characteristics of remotely sensed imageries and particular classes of land cover [12]. Supervised classification method is enormously used for classification of most land cover monitoring [13]. In supervised (maximum likelihood) classification, training samples should be featured as they are essential for assigning brightness values for computer algorithm symbolizing land cover class in each band [14]. In order to apply this method, ground truth should be well known and mind has a set of appropriate categories. Ground truth is characterized with the help of Google Earth. Training samples were drawn on images. Regions of Interest (ROIs) for training samples were selected graphically in irregular polygon shape. They were carefully chosen to be proportion to classes on the output map. Accordingly, maximum likelihood was performed using these ROIs to produce the required thematic map. This operation was performed repeatedly through 13 sub-basins. Because of shortage of spatial coherency in vast majority of classified images, clumping classes was performed to make them smooth. Afterwards, these images were classified to vector to make each class such a single layer to be easily exported to the ArcGIS for preparation the map.

3.5. Accuracy assessment

It is obligatory to provide accuracy assessment in remote sensing technique [15]. The produced classification quality is significant so, information should be provided about it. Error matrix is considered one of the most popular means that represent accuracy assessment [10, 14, 16-18]. It can be defined as a square array of numbers put in the form of rows and columns represent number of training samples that can be either pixels, groups of pixels or polygons set out to definite class relative to the real class (ground truth samples). Overall accuracy, Kappa statistics, user's accuracy and producer's accuracy are classification measures that are commonly used [9]. It is important to estimate the percentage of correct classified pixels and incorrect ones per land cover class on the produced thematic maps, based on Landsat images, prior to authorization the classification results in the final form. In this study, to perform accuracy assessment, other random ROIs were selected on the same Landsat images. They were used as reference data. Environment for Visualizing Image (**ENVI 4.5**) was used to create the error matrix and to derive measures of classification accuracy.

Overall accuracy is an essential classification accuracy measure defined as follows:

$$\text{overall accuracy} = \frac{\text{the sum of major diagonal of matrix (total correct pixels)}}{\text{total number of pixels in the matrix}} \quad (1)$$

Besides overall accuracy, user's accuracy (commission errors) and producer's accuracy (omission errors) are also derived to be used in estimating accuracy.

$$producer's\ accuracy = \frac{the\ number\ of\ correct\ pixels\ in\ a\ class}{\text{total number of column pixels}} \quad (2)$$

where, total column pixels represent the number of total pixels in the ground truth samples (reference data).

$$user's\ accuracy = \frac{\text{total number of pixels of a class}}{\text{total number of row pixels}} \quad (3)$$

Where, total row pixels represent pixels classified in that class.

The kappa statistic is another important technique used for classification accuracy assessment [19]. It is calculated by the following equation:

$$K = \frac{\sum_{i=1}^{r} xii - \frac{1}{N}\sum_{i=1}^{r}(x_{i+} * x_{+i})}{\mathrm{N} - \frac{1}{N}\sum_{i=1}^{r}(x_{i+} * x_{+i})} \quad (4)$$

Where, (r) represents the number of matrix rows, (x_{ii}) represents notices number in row i and column i, (x_{i+}) represents peripheral totals of row i, (x_{+i}) represents peripheral totals of column i and (N) represents total number of notices.

4. Results and discussion

The Abbay Basin was divided into fourteen sub watersheds using 30-m DEM. Satellite images of landsat-8, covering the whole scene of study area, were used. The aimed six land cover classes were water, urban, barren land, forest, grass and agriculture crops. Supervised (maximum likelihood) classification was performed. The resulted land use/ land cover maps are shown in the following figure.

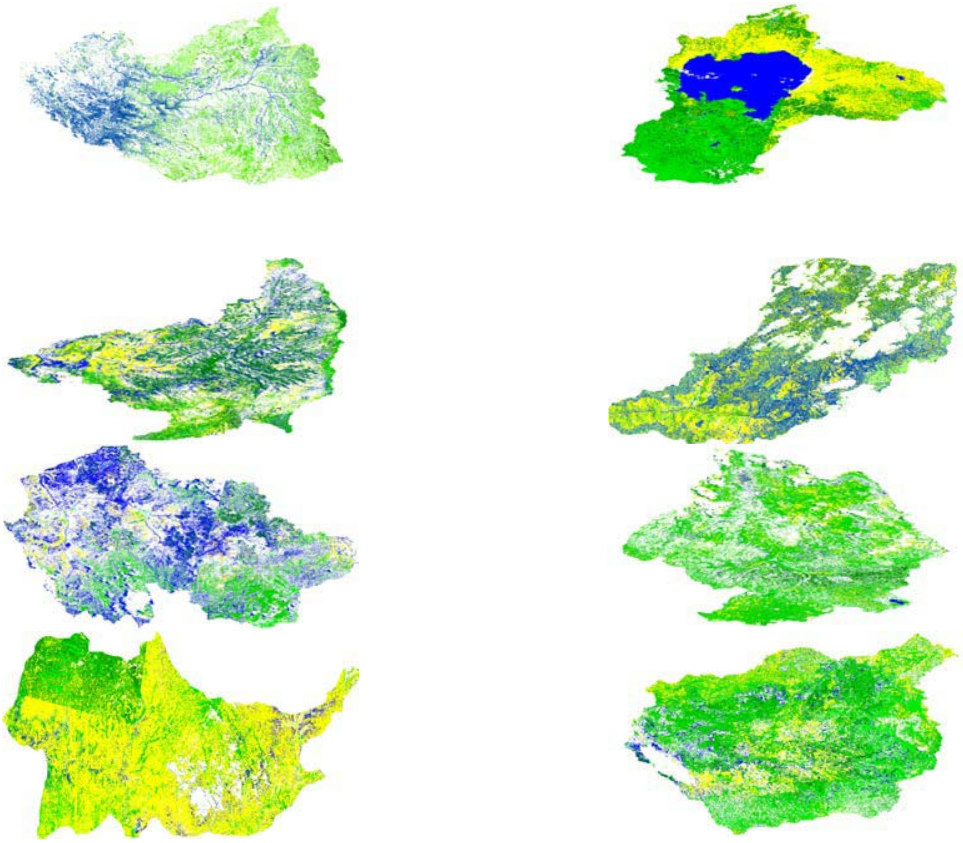

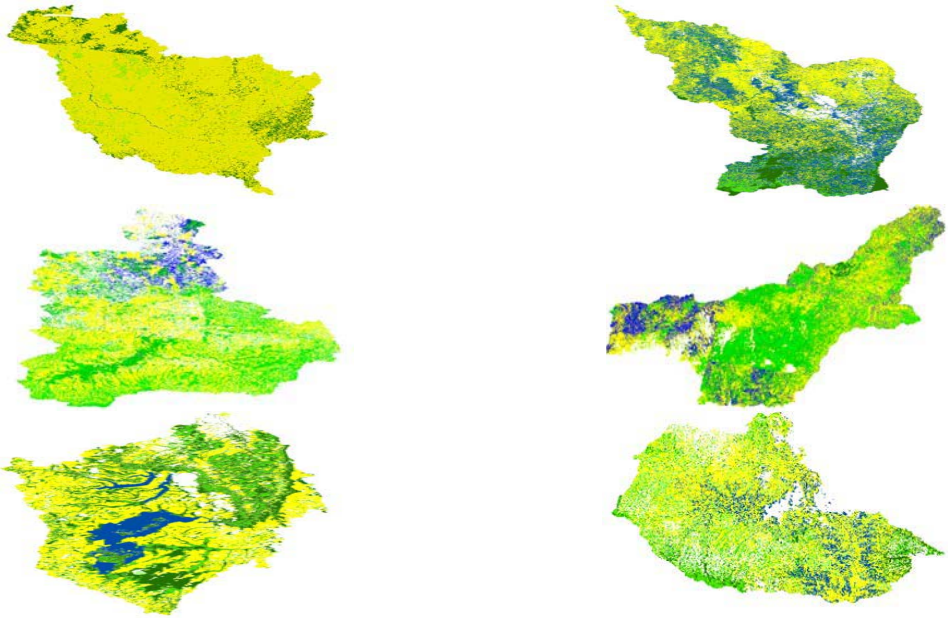

Figure 3 Final resulted land use and land cover maps of whole sub watersheds.

It was found that Weleka and Anger were extracted from images contain clouds cover bigger area compared to clouds in the other images. This makes percentage of urban class in these sub watersheds is large. The following figure shows land sat images of Weleka and Anger sub watersheds.

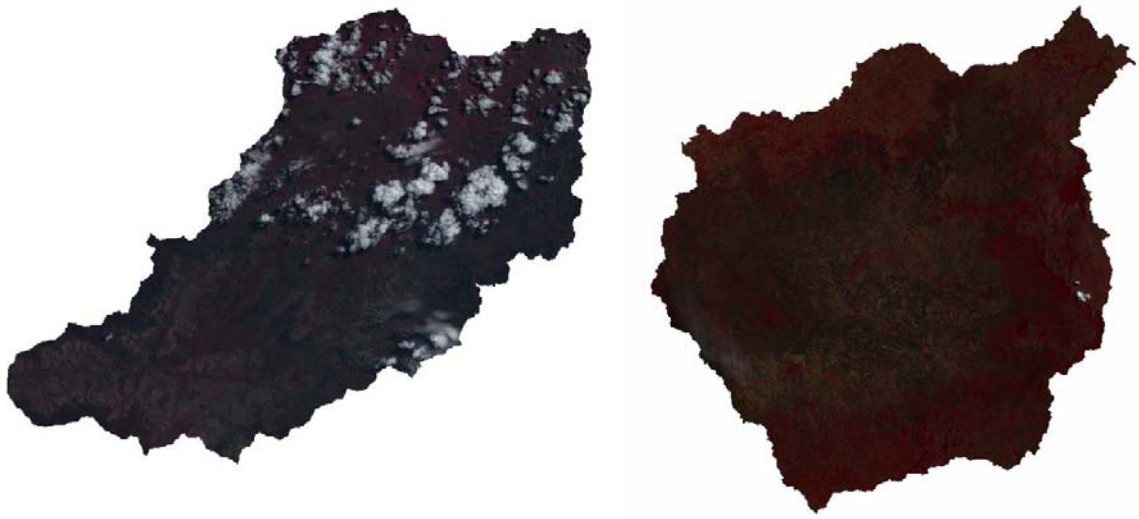

(a) Land sat image of Weleka sub watershed (b) Land sat image of Anger sub watershed

Figure 4 land sat images.

In order to compare easily among the percentages of land cover/ land use of the whole 14 sub watersheds of the Blue Nile basin, please see Table 4.

Table 4 percentage of each class for the whole sub watersheds.

feature / watershed	Water	Urban	Barren	Forest	Grass	Crops
Beshelo	15.66%	50.89%	3.33%	1.16%	7.71%	21.2%
Tana	19.1%	4.25%	29.35%	15.6%	13%	18.55%
Jemma	10.92%	41.91%	12.76%	1.3%	6.3%	26.72%
Weleka	20.67%	32.65%	28.96%	2.32%	5.29%	10.11
Mugger	22.93%	54.5%	4.66%	2.43%	10.32%	5.16%
Guder	1.6%	42.21%	9%	2.22%	37.46%	7.52%
S- Gojam	3.51%	10.88%	60.35%	5.51%	14%	5.75%
Anger	4.33%	26.82%	13.54%	8.1%	40%	7.22%
Wenbera	0.42%	——	86.4%	7.9%	5.28%	——
Didessa	23.5%	18.295	24.31%	17.65%	16.24%	——
Dabus	4%	28.1%	37.1%	18.6%	12.2%	——
Beles	11.9%	7.15%	40.8%	16.65%	21.5%	2%
Fincha	6.63%	12.58%	41.8%	18.44%	18.23%	2.33%
N-Gojam	9.83%	21.13%	37.18%	4.06%	14.66%	13.14%

Figure 5 display the estimated accuracy measures of the watersheds.

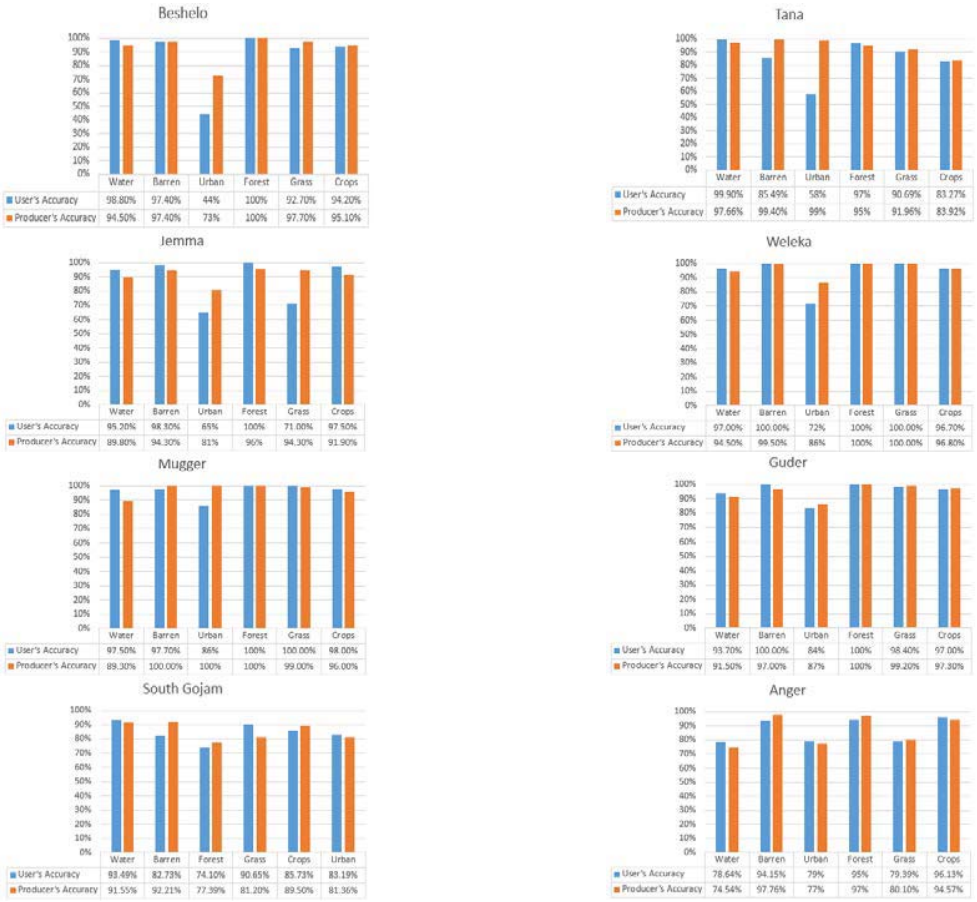

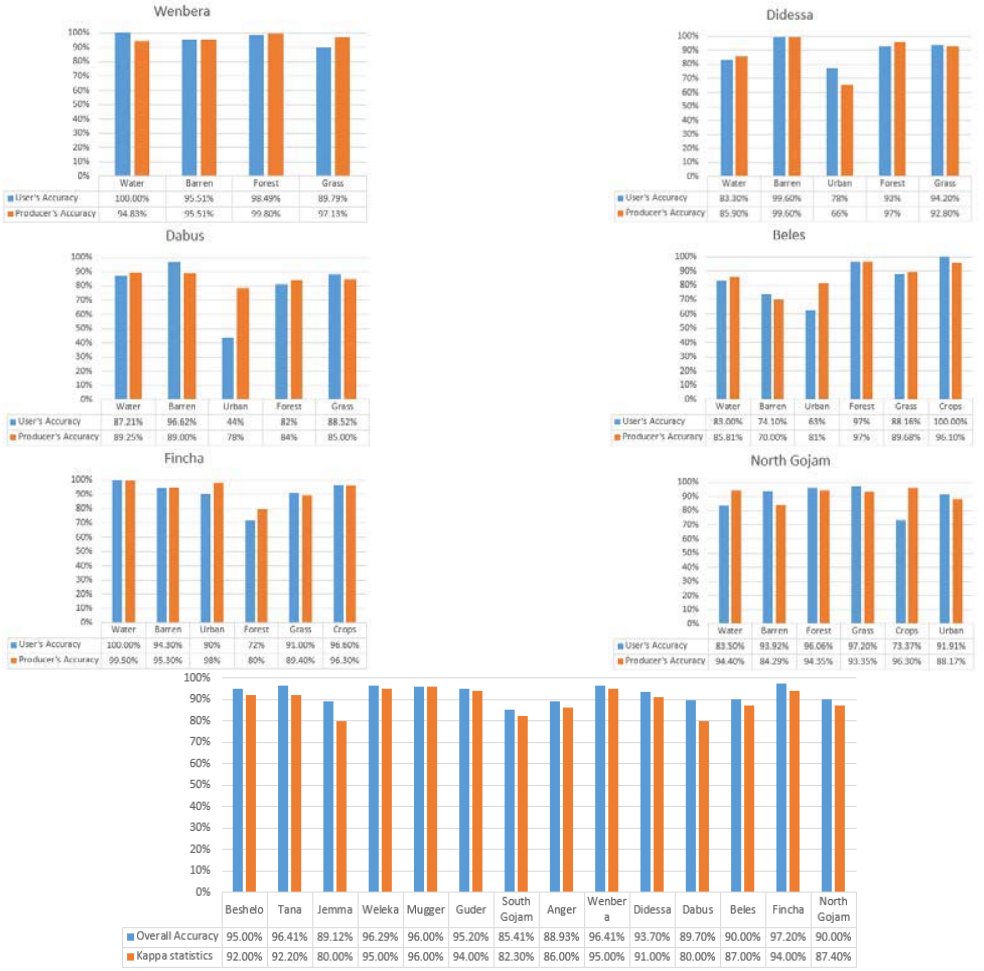

Figure 5 Estimated accuracy measures of the watersheds.

From the previous figure, it was found that the user's and producer's accuracies for all classes, except urban class, are reasonable as they range from 70% to 100%. The user's accuracy for urban class was low in some sub watersheds such Beshelo (44%), Tana (57.9%) and Dabus (44%). Such low accuracies occurred because these sub watersheds were extracted from more than one image at different times unlike the other sub watersheds which were extracted from one image.

5. Conclusions

From this research, we can conclude that:

- Landsat-8 images are the promising choice of satellite image data source because of their low cost and availability of funding.
- As landsat-8 images are available long time image, they can be used for analyzing the change dynamics and updating of land use and land cover.
- Geographic Information System (GIS) is effective in delineating basins as it is the most convenient tool to integrate with remote sensing for mapping.
- The commercial software Environment for Visualizing Images (ENVI) is suitable for image classification process as it can create error matrix and derive measures of classification accuracy.

- Accuracy measures for all sub watersheds are found acceptable except user's accuracy for Beshelo, Tana and Dabus because the images covered these sub watersheds were multi temporal images.

References

[1] Sadek M, Li X, Mostafa E, Freeshah M, Kamal A, Sidi Almouctar M A, Zhao F and Mustafa E K 2020 Low-cost solutions for assessment of flash flood impacts using Sentinel-1/2 data fusion and hydrologic/hydraulic modeling: Wadi El-Natrun Region, Egypt *Advances in Civil Engineering*, Vol. **2020**.
[2] Awulachew S B, Yilma A D, Loulseged M, Loiskandl W, Ayana M and Alamirew T 2007 *Water resources and irrigation development in Ethiopia*, Vol. **123** Iwmi.
[3] Jensen J R 2005 Introductory digital image processinga remote sensing perspective Tech rep.
[4] Yilma A D and Awulachew S B 2009 Characterization and Atlas of the Blue Nile Basin and its Sub basins.
[5] Shahin M M 1985 *Hydrology of the Nile basin, Elsevier*.
[6] Hurst H E and Phillips P 1938 *The hydrology of the Lake Plateau and Bahr el Jebel*, Government Press.
[7] Huffnagel H et al 1961 Agriculture in Ethiopia *Agriculture in Ethiopia*.
[8] Ashour A S, Moussa O M, Al-Tohame F, and El-Hanafy H E 2014 Determination of Grand Ethiopian Renaissance Reservoir (GERR) Life Span Using Remote Sensing Techniques *The International Conference on Civil and Architecture Engineering* Vol. **10** Military Technical College pp. 1–28.
[9] Wondrade N, Dick Ø B, and Tveite H 2014 GIS based mapping of land cover changes utilizingmulti-temporal remotely sensed image data in Lake Hawassa Watershed, Ethiopia *Environmental monitoring and assessment* Vol. **186** No. 3 pp. 1765–1780.
[10] Congalton R G A 1991 review of assessing the accuracy of classifications of remotely sensed data *Remote sensing of environment* Vol. **37** No. 1 pp. 35–46.
[11] Anderson J R 1976 A land use and land cover classification system for use with remote sensor data US Government Printing Office Vol. **964**.
[12] Aplin P 2004 Remote sensing: land cover *Progress in Physical Geography* Vol. **28** No. 2 pp. 283–293.
[13] Rogan J and Chen D 2004 Remote sensing technology for mapping and monitoring land-cover and land-use change *Progress in planning* Vol. **61** No. 4 pp. 301–325.
[14] Lo C and Yeung A 2002 Concepts and techniques of geographic information systems.
[15] Okeke F and Karnieli A 2006 Methods for fuzzy classification and accuracy assessment of historical aerial photographs for vegetation change analyses. Part I: Algorithm development *International journal of remote sensing* Vol. **27** No. 1 pp. 153–176.
[16] Congalton R G, Green K et al 2009 Assessing the accuracy of remotely sensed data.
[17] Foody G M 2002 Status of land cover classification accuracy assessment *Remote sensing of environment* Vol. **80** No. 1 pp. 185–201.
[18] Lillesand T and Kiefer R W 2000 Remote sensing and image interpretation.
[19] Congalton R G 2001 Accuracy assessment and validation of remotely sensed and other spatial information *International Journal of Wildland Fire* Vol. **10** No. 4 pp. 321–328.